Climate Dynamics (2019) 53:4521–4537
https://doi.org/10.1007/s00382-019-04802-4

AMOC sensitivity to surface buoyancy fluxes: the role of air-sea feedback mechanisms

Yavor Kostov[1] · Helen L. Johnson[2] · David P. Marshall[1]

Received: 16 September 2018 / Accepted: 3 May 2019 / Published online: 20 May 2019

Abstract
We interrogate the sensitivity of the Atlantic Meridional Overturning Circulation (AMOC) to surface heat and freshwater fluxes over the Subpolar Gyre in an ocean general circulation model and its adjoint. Surface heat loss out of the Subpolar Gyre in the winter strengthens the AMOC at a lead time of approximately 6 months. However, the same surface heat flux anomaly in the summer leads to a delayed AMOC weakening that emerges at a lag of 8 months. Under a summer surface cooling perturbation, the AMOC progressively weakens up to a lag of approximately 80 months, and then the negative overturning anomaly persists for years. Compared with the sensitivity to surface heat fluxes, seasonality in the AMOC sensitivity to surface freshwater fluxes is less pronounced, and there is no sign reversal between the response to summer and winter perturbations. We explain the mechanisms behind the large seasonal differences in the AMOC sensitivity to surface heat fluxes and highlight the role of evaporation. Heat flux anomalies over the Subpolar Gyre trigger changes in the rate of evaporation and hence affect the salinity of the mixed layer. Surface cooling gives rise to freshening in the following months, whereas warming leads to salinification. Persistent buoyancy changes due to salinity responses counteract the impact of heat fluxes to a varying extent depending on the seasonal mixed layer depth. On the other hand, air-sea feedback mechanisms exert a positive feedback on the AMOC response to surface freshwater flux perturbations both in the summer and in the winter months.

Keywords North Atlantic · Meridional overturning circulation · Surface heat flux · Surface freshwater flux · Seasonality · Sensitivity · Mixed layer

1 Introduction

The Atlantic meridional overturning circulation (AMOC) transports approximately 0.5 PW of heat northward across the Equator (Buckley and Marshall 2016) and impacts regional and global climate (Stolpe et al. 2018). The circulation is implicated as one of the possible factors that keep Western European winters mild compared to other parts of the Northern Hemisphere [e.g., Seager et al. (2002)]. The AMOC also plays an important role in the surface uptake and vertical distribution of heat and carbon within the ocean (Kostov et al. 2014; Marshall et al. 2014; Stolpe et al. 2018; Winton et al. 2013). This in turn affects the evolution of surface climate under greenhouse gas and aerosol forcing (Kostov et al. 2014). On the other hand, the AMOC itself responds to anthropogenic and natural variability in the atmosphere (Winton et al. 2013). For example, the maximum strength of overturning is projected to decline during the 21st century because of increasing heat and freshwater fluxes into the North Atlantic (Cheng et al. 2013; Gregory et al. 2005; Meehl et al. 2013; Rugenstein et al. 2013). The resulting circulation anomaly is expected to redistribute the ocean's reservoir of heat and carbon (Winton et al. 2013).

Because of the AMOC's outstanding importance for large-scale ocean and climate variability, a number of theoretical and modeling studies have explored the sensitivity of the circulation to surface buoyancy forcing at different latitudes, as well as the meridional transport connectivity (Zou et al. 2019) in the Atlantic Ocean, i.e., the extent to which AMOC anomalies are causally related across different latitudes. Observational arrays that estimate the strength of the AMOC have been set up at various latitudes such as 26°N [the RAPID-MOCHA line, e.g., Smeed et al. (2014)],

✉ Yavor Kostov
yavor.kostov@physics.ox.ac.uk

[1] Clarendon Laboratory, Department of Physics, University of Oxford, Parks Road, Oxford OX1 3PU, UK

[2] Department of Earth Sciences, University of Oxford, Oxford OX1 3AN, UK

as well as across the eastern and western Subpolar Gyre [the OSNAP East and West arrays, e.g., Lozier et al. (2017)]. Bugnion et al. (2006b) and Yeager and Danabasoglu (2014) point out the importance of buoyancy forcing in the subpolar North Atlantic and its marginal seas for the long-term variability of the AMOC at lower latitudes. However, the meridional connectivity in the North Atlantic need not translate into a meridional coherence of anomalies in AMOC strength and spatial structure (Lozier 2010). Moreover, a strong north-south connectivity along the Western Boundary of the North Atlantic does not necessarily imply a direct advective pathway between the Subpolar and the Subtropical Gyre. Zou and Lozier (2016) suggest that particles released in the Subpolar Gyre tend to recirculate or follow interior ocean pathways. On the other hand, wave propagation along the continental shelves provides an alternative or complementary non-advective mechanism that facilitates the north-south connectivity along the Western Boundary (Johnson and Marshall 2002; Kawase 1987; Zhang 2010) and the south-north connectivity along the Eastern Boundary (Jones et al. 2018) thereby supporting oceanic teleconnections between the Subpolar Gyre and the subtropics.

Here we analyze the monthly to decadal response of the subtropical AMOC at 26°N (the RAPID-MOCHA line) to surface heat and freshwater fluxes over the Subpolar Gyre. We use the MIT general circulation model (MITgcm, Marshall et al. 1997a, b) and its adjoint (Giering 2010; Heimbach et al. 2011; Pillar et al. 2016), as well as an offline mixed layer process model to highlight the importance of local air-sea feedback mechanisms. We show that the representation of surface boundary conditions strongly affects the RAPID-AMOC sensitivity to thermohaline forcing over the Subpolar Gyre.

A number of studies emphasize the importance of appropriately representing surface boundary conditions when modeling AMOC variability. Relaxing surface temperature and/or salinity to prescribed values is a common approach because it reduces model drift. Griffies and Tziperman (1995) used an idealized box model to demonstrate that different damping timescales of temperature and salinity influence AMOC variability. Arzel et al. (2006) also highlighted the importance of temperature relaxation for the multidecadal variability of the AMOC.

In contrast, in our model-based study, we do not restore sea surface temperature or salinity, but instead we employ either parameterized or fully prescribed heat and freshwater fluxes as our boundary conditions. The bulk formulae, atmospheric fields, and surface fluxes that we apply in our numerical experiments are consistent with the ECCO historical assimilation (Forget et al. 2015; Fukumori et al. 2017) which is constrained by ocean observations and atmospheric reanalysis. Using boundary conditions based on ECCO allows us to explore the impact of air-sea feedback mechanisms on the AMOC in a more realistic framework compared to model configurations that rely on prescribed surface restoring conditions.

Section 2 presents further details about our methods and numerical experiments. Section 3 describes the results of our forward and adjoint calculations. Section 4 discusses our findings and summarizes the importance of air-sea feedback mechanisms for the RAPID-AMOC sensitivity to surface heat and freshwater fluxes into the Subpolar Gyre.

2 Data and methods

In this study we use an ocean-only configuration of the MITgcm (Marshall et al. 1997a, b) general circulation model (GCM) that represents the global domain at a nominal 1×1 degree resolution and includes an Arctic Ocean. The model grid approaches a latitude-longitude coordinate system at low latitudes but diverges away from this regular topology at high latitudes. To avoid a singularity at the geographical North Pole, the grid has four Arctic poles located on land. The model configuration includes a Gent-McWilliams (GM) eddy parameterization based on Griffies (1998), a GGL90 turbulent kinetic energy (TKE) vertical mixing scheme (Gaspar et al. 1990), and an interactive sea ice representation. These computational schemes are tuned with parameter values based on the ECCO optimization (Forget et al. 2015; Fukumori et al. 2017). As discussed in Sect. 1, we do not restore SST and surface salinity to climatological values; instead we use surface fluxes as a boundary condition for the ocean and sea-ice domain. We initialize the ocean state with realistic conditions based on the ECCO state estimate and drive the model with optimized time-evolving historical atmospheric forcing available from ECCO (Forget et al. 2015; Fukumori et al. 2017). As part of the optimization process, the surface forcing fields have been adjusted to minimize the discrepancy between the ocean state estimate and observations. The ocean-only model uses bulk formulae to parameterize surface heat and freshwater fluxes as a function of SST, prescribed time-evolving atmospheric conditions, and external radiative forcing. External forcing and atmospheric conditions are applied with a 6-hourly temporal resolution.

To obtain the adjoint of the ocean-only MITgcm (Heimbach et al. 2011) and compute the AMOC sensitivities to surface buoyancy fluxes linearized about the time-evolving model background state, we use TAF, a proprietary algorithmic differentiation software (Giering 2010). We start by evaluating a given objective function (such as the strength of the AMOC) in a forward model simulation. We then perform our adjoint analysis to obtain the first derivatives of that objective function with respect to various model inputs (Pillar et al. 2016). These derivatives represent the linear

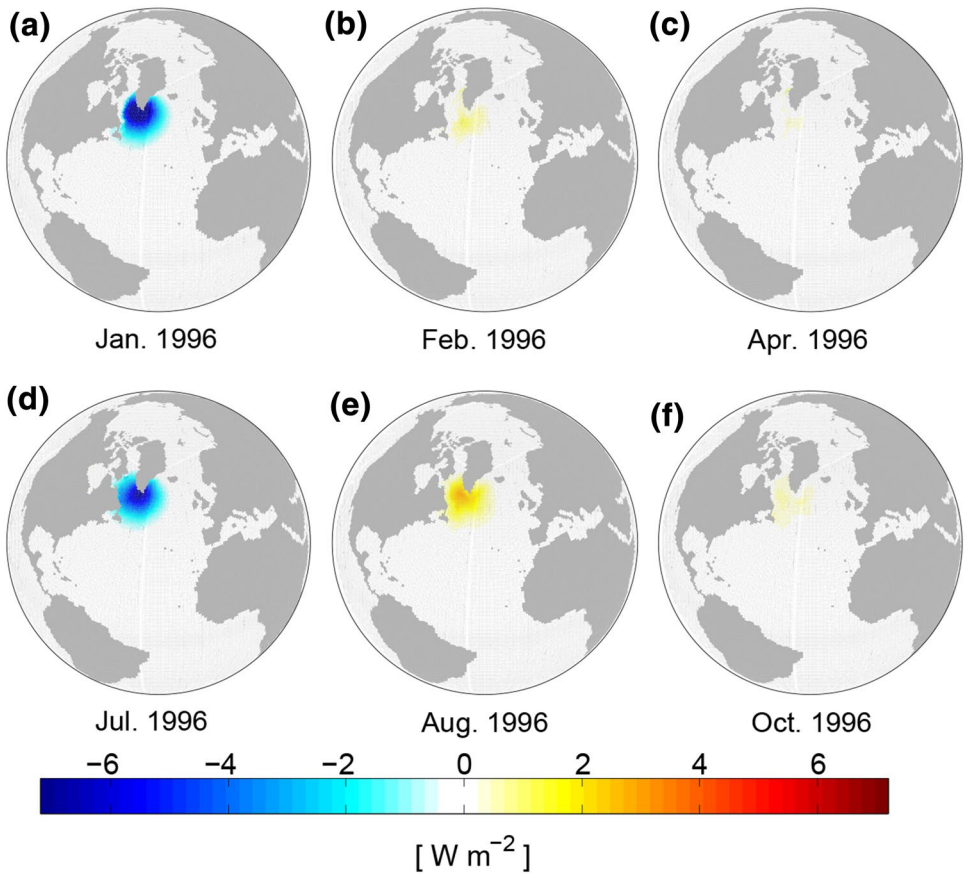

Fig. 1 **a** Imposed cooling perturbation to the surface heat flux into the ocean [W/m^2] sustained throughout January 1996 of the simulation; **b** freely evolving surface heat flux anomaly at a lag of +1 month; **c** as in b for a lag of +3 months; **d**–**f** same as **a**–**c** but for a heat flux perturbation applied in July 1996

sensitivities of the objective function. In our adjoint calculations, we consider objective functions defined as the monthly-averaged overturning at 26°N both in depth space and in potential density space referenced to 1000 dbar. In depth space we compute the integrated northward volume transport in the Atlantic ocean, across 26°N, and above the climatological annual-mean depth of the AMOC streamfunction maximum (1100 m in the model). Our objective function in potential density space is similarly defined as the northward volume transport across 26°N in all potential density classes in the Atlantic Ocean lighter than 1032.1 kg m^{-3} (the climatological maximum of the density-space AMOC in our model). We evaluate our objective functions in February 2006 of the ECCO historical simulation, 15 years into the model run. However, we have also performed calculations with objective functions evaluated in other months of the year, and the sensitivities we calculate are not affected substantially (not shown).

As the AMOC changes between different periods of the simulation, variations in the objective function may be expected depending on the year chosen to evaluate it. In our case, this is the year 2006. Similarly, when we perform forward perturbation experiments (see below), we apply a forcing anomaly in a particular time period from the historical simulation: either January or July 1996. Both years, 1996 and 2006, are chosen as fairly representative of the time-mean North Atlantic conditions in the simulation. In 1996 and in 2006, the mixed layer depth in the subpolar North Atlantic is smaller compared to the early 1990s marked by very strong deepwater formation, and larger compared to the late 1990s marked by a very shallow mixed layer (not shown).

In addition to the adjoint calculations, we perform a set of forward perturbation experiments with the same configuration of the MITgcm. We first apply a short-lived (1 month long) perturbation to the surface downwelling longwave radiation in January 1996 of the ECCO historical simulation. The simulation starts in 1992, but we branch off our perturbation experiments in 1996 (because convection in the North Atlantic marginal seas is unusually strong earlier in the 1990s, as discussed earlier). The spatial pattern of the imposed perturbation is a Gaussian that is centered off the southern tip of Greenland and encompasses the Subpolar Gyre (Fig. 1a). The perturbation has a peak amplitude of 10 W/m^2, which is comparable to the typical variability in monthly-mean July surface heat fluxes over the Subpolar Gyre across the 20 years of the ECCO assimilation (see Fig. 11 in Appendix 1). We then conduct a similar experiment where we impose the same heat flux anomaly in July 1996. We furthermore perform analogous

experiments with perturbations to the surface freshwater flux over the Subpolar Gyre in January and in July 1996. Our freshwater flux perturbations have the same Gaussian spatial pattern as our heat flux perturbations.

In order to test the dependence on feedback mechanisms, we repeat the set of adjoint and forward calculations in a model configuration where the surface heat and freshwater fluxes are fully prescribed using monthly-averaged values based on the ECCO simulation. Thus, the surface fluxes in these additional experiments are not allowed to respond to the sea surface temperature (SST) anomalies arising from our prescribed surface forcing. We use the time-evolving surface fluxes at the ocean liquid interface as diagnosed from the historical ECCO simulation. The use of monthly rather than hourly resolution in the forcing leads to small deviations in the evolution of the simulated AMOC strength at 26°N relative to the original ECCO simulation that has active air-sea feedback.

However, in this calculation with fully prescribed monthly-mean surface fluxes, the model exhibits a large SST drift in the Subpolar North Atlantic. This change in the background model state impacts the sensitivity to surface fluxes. There are several factors that explain this drift. Taking monthly averages artificially eliminates some of the covariability between heat and freshwater fluxes on shorter timescales, contributing to a drift in the circulation. In addition, large variability on timescales shorter than a month plays an important role in the high latitudes as it impacts the rate of deep convection in the winter, and consequently, the overturning transport throughout the Atlantic. For example, Holdsworth and Myers (2015) show that removing high-frequency variability in atmospheric forcing can reduce the strength of the AMOC by 25%. In our study, when we prescribe the monthly mean net surface fluxes, the resulting large drift in the subpolar North Atlantic biases our linear sensitivity analysis because it is performed relative to a drifting model trajectory.

In order to avoid any model drift or deviation from the original ECCO historical simulation, we also consider a third approach. When computing the cost function, we keep the parameterized surface fluxes exactly as in ECCO. We thus maintain the same ocean background conditions as in the original historical simulation. However, we do not algorithmically differentiate the surface flux parameterization routines in the adjoint calculation. In other words, we leave out the contribution of the bulk formulae to the linear sensitivity of the AMOC to surface heat and freshwater fluxes. This approach guarantees that when we compute our AMOC cost function, there is no model drift relative to the ECCO forward trajectory. At the same time, our approach removes the impact of local air-sea feedback on the AMOC sensitivity. In this case, the adjoint of the model treats surface heat and freshwater fluxes as if they were purely external forcing, independent of SST anomalies.

3 Results

We first analyze the adjoint-based sensitivity of the AMOC to surface heat and freshwater fluxes in a model configuration with bulk forumulae parameterizations. At short lead times, an input of heat or freshwater into the Subpolar Gyre triggers a fast barotropic redistribution of volume (Pillar et al. 2016). At lead times longer than a year, there is a seasonal sign reversal in the sensitivity to heat fluxes averaged over the Western Subpolar Gyre region, 42°N to 67°N and 65°W to 30°W (Fig. 2a, blue). This result suggests that both winter heat loss and summer heat gain over the Labrador Sea can cause a delayed strengthening of the subtropical AMOC. The maximum AMOC strengthening in response to a summer heat loss is expected at a lag of approximately 80 months. The seasonal sign reversal in heat flux sensitivity is not mirrored in the corresponding sensitivity to regional surface freshwater fluxes (Fig. 2b, blue, and Fig. 2c for heat and freshwater fluxes scaled in the same units). We obtain almost identical sensitivity results when we define the AMOC strength in density space (not shown). In our further discussion of adjoint calculations we refer to the results in depth space.

Buoyancy forcing over the Subpolar Gyre influences the AMOC at 26°N via two distinct mechanisms: propagation of density anomalies as boundary waves and advection (Zhang 2010). We subsequently focus on sensitivities at a lead time of 5 years corresponding to a slow multiannual advective timescale [e.g. Zhang (2010)]. We find that both the heat and the freshwater flux sensitivity exhibit consistent north-south dipole patterns in winter months (Fig. 3). The dipole pattern indicates a positive sensitivity of the 26°N AMOC to buoyancy loss in the Subpolar Gyre and buoyancy gain in the subtropics. The maps of sensivity to surface heat fluxes (Fig. 3a–c) show a clear seasonal sign reversal in the Subpolar Gyre that has no counterpart in the sensitivity to freshwater input (Fig. 3d–f).

We explore how historical variability in the ECCO surface heat fluxes projects onto the AMOC sensitivity maps at various lead times. We focus on the the Western Subpolar Gyre region, 42°N to 67°N and 65°W to 30°W and mask the rest of the World Ocean. We multiply each of our sensitivity patterns by a 1 standard deviation surface heat flux anomaly relative to the climatological monthly mean, as estimated from the ECCO historical simulaiton. Our analysis suggests that a typical heat flux anomaly in July, sustained over 1 month, is expected to give rise to an order 0.001 Sv change in the AMOC at a lag of several years. In contrast, a typical January heat flux anomaly gives rise to a ~ 0.03 Sv linear

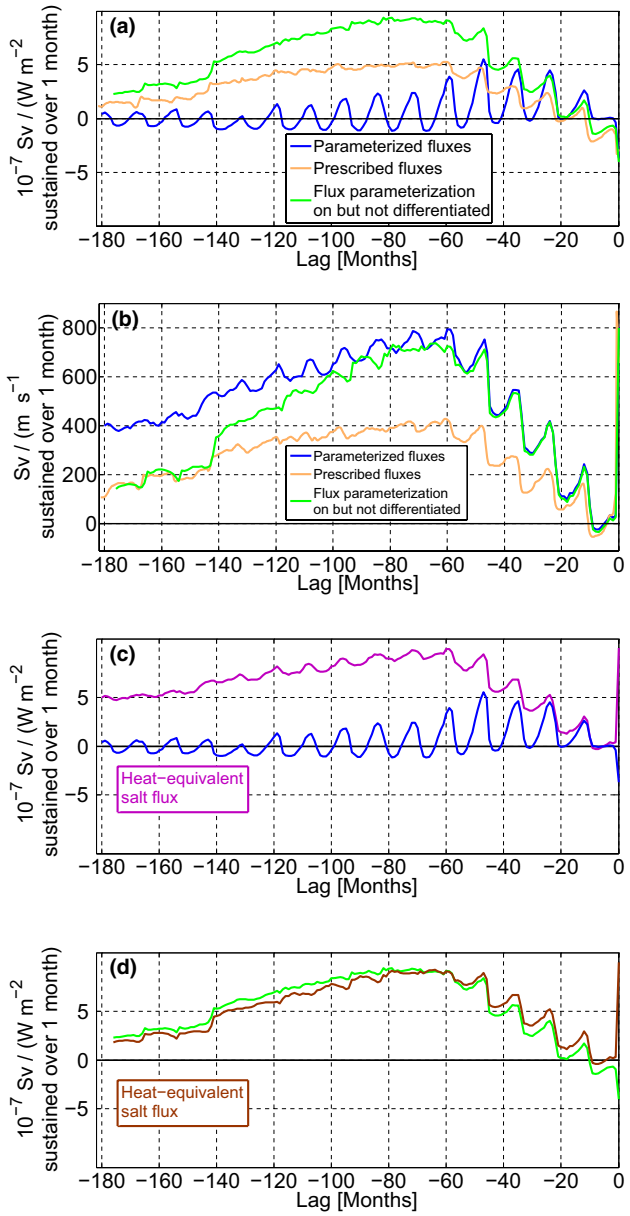

Fig. 2 **a**, **b** Lagged sensitivity of the AMOC to surface buoyancy fluxes integrated over the Western Subpolar Gyre region between 42°N to 67°N and 65°W to 30°W: **a** sensitivity to surface heat fluxes out of the ocean [Sv per (W/m^2 sustained over 1 month)]; **b** sensitivity to evaporation minus precipitation [Sv per (m/s sustained over 1 month)]. Blue curves: monthly means of the sensitivity from a simulation with parameterized surface fluxes; orange: same as blue but from a model configuration with fully prescribed surface heat and freshwater fluxes. Green: same but for an experiment where the original surface flux parameterizations are active in the forward calculation but are not differentiated in the adjoint calculation of linear sensitivity. **c** Same as the blue curves from **a** and **b** but the sensitivity to freshwater fluxes (magenta) is rescaled to be in the same units as the sensitivity to heat fluxes (blue) [Sv per (W/m^2 sustained over 1 month)]; **d** Same as the green curves from **a**, **b** but the sensitivity to freshwater fluxes (brown) is rescaled to be in the same units as the sensitivity to heat fluxes (green) [Sv per (W/m^2 sustained over 1 month)]

AMOC response. However, we point out that our adjoint sensitivity patterns do not fully capture nonlinear processes that amplify the AMOC response (see Appendix 3 for a discussion of nonlinearity).

3.1 Sensitivity of the AMOC to surface heat fluxes over the subpolar gyre

To what extent is this seasonality in the AMOC sensitivity to surface heat fluxes influenced by air-sea feedback mechanisms? We repeat the adjoint calculation with time-evolving but fully prescribed historical surface heat and freshwater fluxes based on monthly averaged values from the original ECCO simulation. These prescribed surface fluxes are not allowed to adjust to SST. In other words, there is no SST feedback on air-sea heat exchange or on evaporation. In this case, the seasonal sign reversal in the sensitivity to surface heat fluxes disappears (Fig. 2a, orange).

Some of the difference between the adjoint calculations with prescribed versus parameterized fluxes is due to model drift in the North Atlantic, as discussed in Sect. 2. A third approach allows us to avoid this issue. We perform an additional experiment where we maintain the original surface flux parameterization in the forward simulation that provides our model background conditions. However, we do not differentiate the bulk formulae and radiation routines in the adjoint calculation. Without the contribution due to parameterized surface feedback, the linear AMOC sensitivity to surface heat fluxes is now characterized by a spatial pattern resembling more closely the sensitivity to salinity (not shown). Moreover, the sensitivity to surface heat fluxes averaged over the subpolar gyre no longer exhibits a seasonal sign reversal (Fig. 2a, green and Fig. 2d for heat and freshwater fluxes scaled in the same units).

At lead times longer than two years, the sensitivity to surface heat fluxes is noticeably larger in magnitude than the original result from the configuration with bulk formulae contributions. We can understand this in terms of the negative feedback that the surface flux parameterization exerts on the heat anomalies in the upper ocean. For example, a positive SST anomaly leads to an increase in parameterized upwelling longwave radiation, as well as an increase in sensible and latent heat fluxes out of the ocean. When we eliminate this feedback mechanism, our sensitivities no longer include a contribution from the damping of mixed layer heat anomalies to the atmosphere. Hence, the sensitivities to heat fluxes decay more slowly at long lead times compared to the case with bulk formulae contributions. This is similar to the results of Pillar et al. (2016), who consider a model configuration with fully prescribed surface fluxes and find non-negligible annual-mean sensitivities to surface heat uptake at a lead time of 9 years. Our results are also consistent with Bugnion et al. (2006a) and Czeschel et al. (2010)

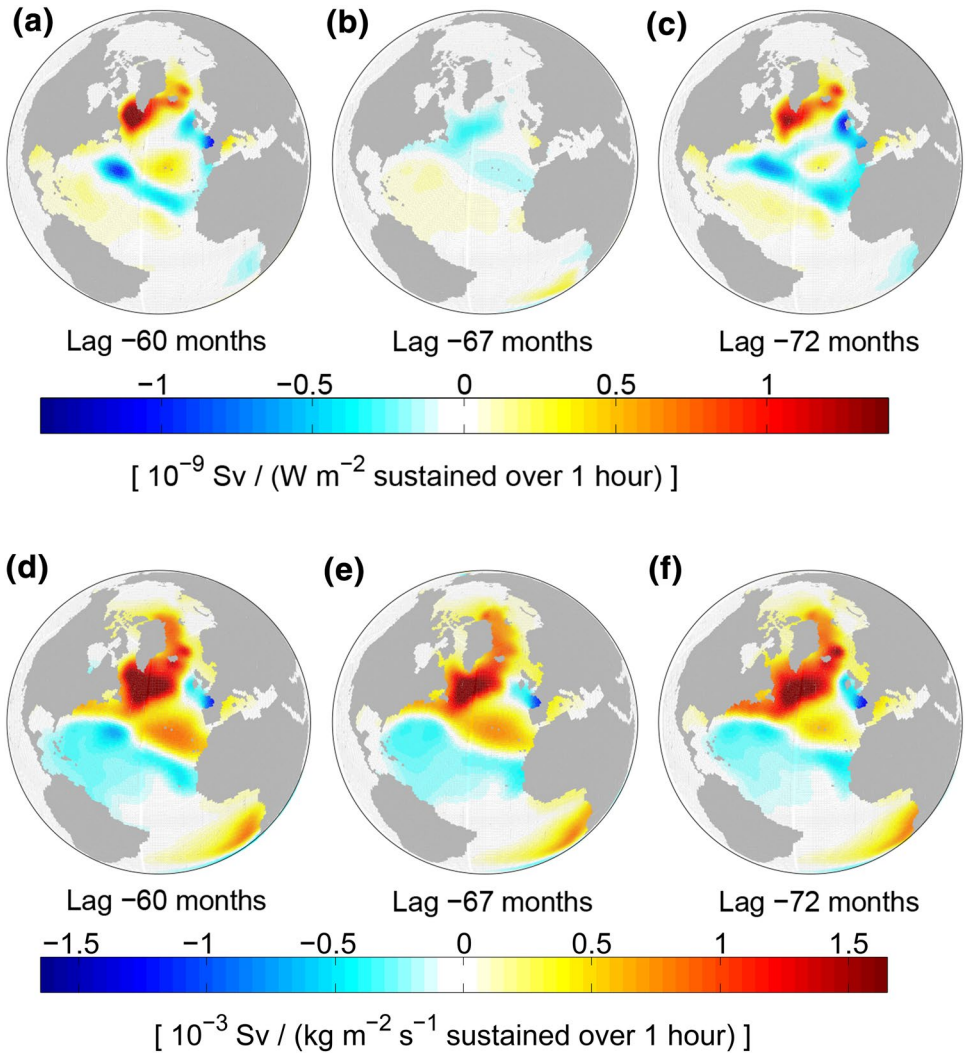

Fig. 3 **a–c** Sensitivity of the AMOC to parameterized surface heat fluxes out of the ocean [Sv per (W/m^2 sustained over 1 h)] if the heat fluxes are applied in **a** January at a lead time of 60 months; **b** August at a lead time of 67 months; **c** January at a lead time of 72 months; **e–f** same as a-c but for the sensitivity to evaporation minus precipitation [Sv per (kg m^{-2} s^{-1} sustained over 1 hour)]. Red (blue) shading indicates that the AMOC strengthens in response to a hypothetical positive (negative) flux anomaly at the specified lead time. The sensitivities were smoothed using a diffusive Gaussian operator with a spatial scale of 3 grid points after Weaver and Courtier (2001)

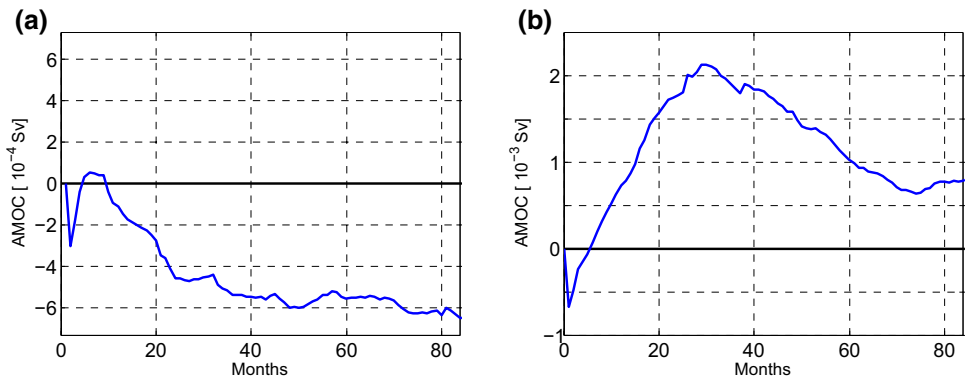

Fig. 4 Lagged response of the AMOC at 26°N to a surface heat flux perturbation (cooling) applied in **a** July and **b** January 1996

who find much larger AMOC sensitivity to surface buoyancy fluxes under fully prescribed surface fluxes than under restoring boundary conditions, which represent an effective damping of heat anomalies to the atmosphere.

Forward experiments with imposed surface heat flux anomalies over the Subpolar Gyre (Fig. 1) confirm the presence of a seasonal sign reversal in the AMOC sensitivity and shed light on the role of air-sea feedback mechanisms. For example, we demonstrate that summer cooling over the Subpolar Gyre can lead to a delayed weakening rather than a strengthening of the subtropical AMOC (Fig. 4) consistent with the sign of the response in our adjoint sensitivity

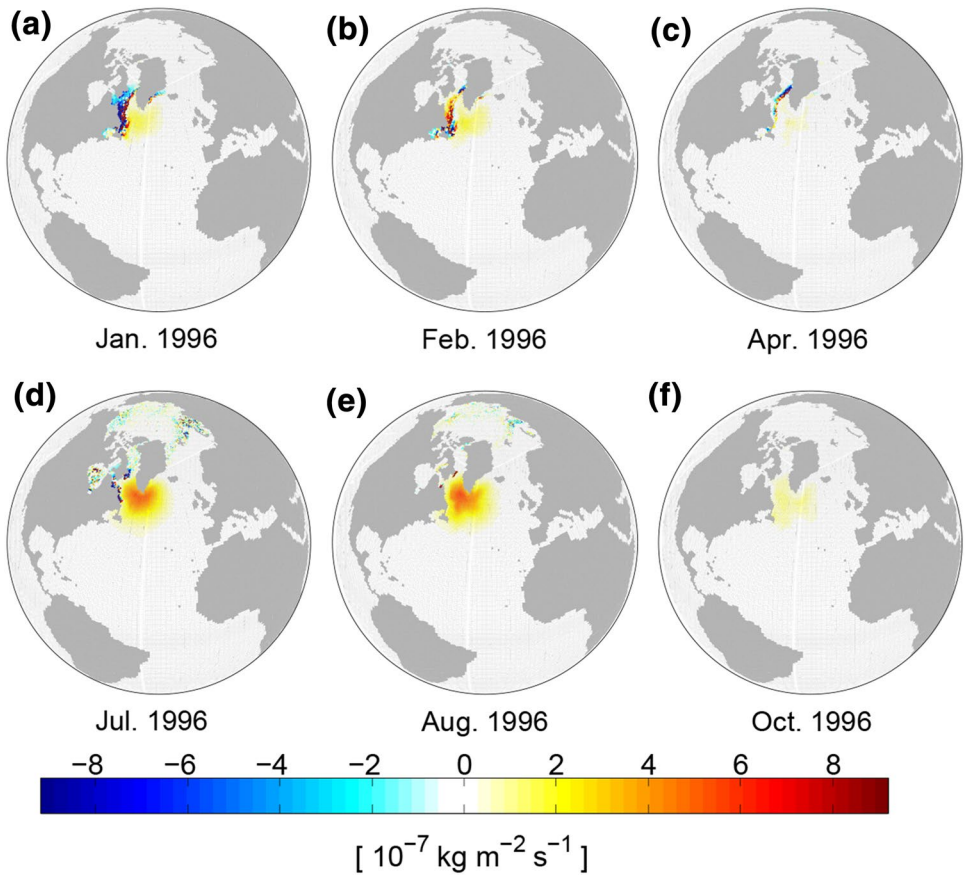

Fig. 5 Response of the freshwater flux into the ocean [kg/m^2/s] to a surface heat flux perturbation (cooling) applied in January 1996 (Fig. 1a). Response at **a** zero lag; lag of **b** +1 month; **c** +3 months; **d**–**f** same as **a**–**c** but for the response of the freshwater flux to a heat flux perturbation (cooling) applied in July 1996 (Fig. 1d)

calculations. The perturbations we apply are deliberately small (with a peak amplitude of 10 W/m^2) in order to explore the linear regime captured by the adjoint calculation.

Our results show that the surface heat content anomaly is more strongly damped by the atmosphere in the summer months compared to the winter months (Fig. 1b–f). At the same time, the freshwater fluxes respond more strongly to surface heat fluxes in the summer than in the winter (Fig. 5). The seasonality in surface freshwater flux responses is partially enhanced by greater sea-ice formation and brine rejection in the winter experiment (not shown). However, the sea-ice contribution to the salinity budget is narrowly confined to the coastal areas of the Labrador Sea and the mouth of Baffin Bay. In contrast, the large surface freshwater flux signal in the interior of the basin (Fig. 5d, e) is due to evaporation responses over the open ocean that exhibit pronounced seasonality. Surface cooling in the summer triggers a larger reduction in evaporation than in winter and ultimately results in freshening of the North Atlantic. We thus identify seasonal differences in the extent to which salinity responses counteract the impact of surface cooling on the density budget of the Subpolar Gyre.

Are these differences in the local air-sea feedback response sufficient to explain the seasonal sign reversal in the surface heat flux sensitivity, or do dynamical processes in the ocean play a dominant role? To address this, we focus on the generation of the density anomaly in the subpolar North Atlantic that is subsequently communicated southward to 26°N via waves and advection. We turn our attention to the experiment where we have perturbed the summer heat fluxes over the Subpolar Gyre. The resulting temperature and salinity anomalies are distributed vertically and horizontally. However, they remain largely confined to the Subpolar Gyre on a timescale of several months. These results sugest that on such short inter-seasonal timescales, between the summer and the winter, the buoyancy anomalies are modulated primarily by local-air sea fluxes rather than by the ocean circulation (Fig. 6).

In order to explore the mechanisms that are dominant on these timescales, we use a process model of the Subpolar Gyre mixed layer without any ocean dynamics. This simplified model assumes a horizontally and vertically homogeneous, uniformly mixed layer with a depth h that increases exponentially in time from 25 m at the end of July to 100 m at the end of December—our process model simuations do not extend beyond a few months. Motivated by the results shown in Fig. 6, we assume that on these timescales, the anomalies in the mixed layer of the Subpolar Gyre are isolated from the rest of the ocean. Therefore, when setting

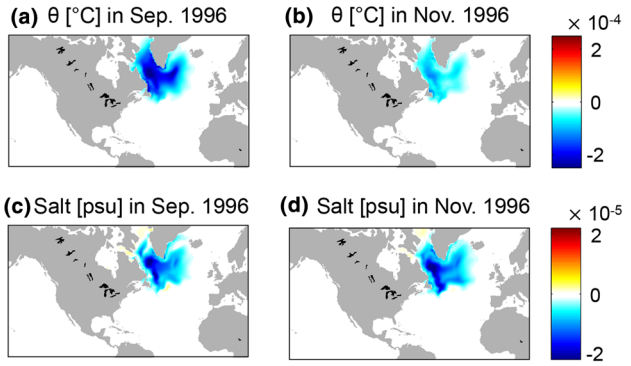

Fig. 6 Vertically averaged anomalies in potential temperature (**a**, **b**) and salinity (**c**, **d**) for the entire water column at two- and four-month time lags after a heat flux perturbation applied in July 1996 (Fig. 1d) of the simulation with active SST feedback on surface fluxes

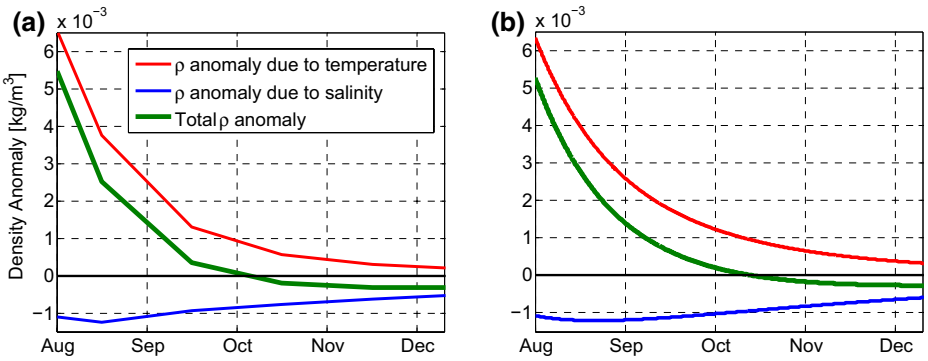

Fig. 7 Contributions to the density anomaly in the upper 30 m of the Western Subpolar Gyre: **a** in the July 1996 heat flux experiment (Fig. 1d); **b** in a process model of the Subpolar Gyre mixed layer forced with initial conditions based on the July 1996 heat flux experiment in **a**. Red: density anomaly due to temperature; Blue: density anomaly due to salinity; Green: total density anomaly

up our process model, we ignore transport by the ocean circulation.

This idealized Subpolar Gyre mixed layer is forced with parameterized surface fluxes using the same bulk formulae as in the MITgcm. In the bulk formulae, we prescribe seasonally representative atmospheric temperature and humidity based on the boundary conditions of the historical ECCO assimilation. We initialize the temperature T and salinity S of our offline process model using values from our MITgcm experiments. Surface fluxes respond to the mixed layer temperature and feed back on the heat and salt budgets:

$$\frac{dT}{dt} = \frac{Q(T)}{C \cdot h(t)} \tag{1}$$

$$\frac{dS}{dt} = -\frac{F(T)}{h(t)} \tag{2}$$

$$\rho = f(T, S, p), \tag{3}$$

where Q and F are the surface heat and freshwater fluxes parameterized as functions of T. Constant C relates the mixed layer heat capacity to the volume. Since we consider only the time period between the end of July and the beginning of December, the mixed layer depth $h(t)$ continuously grows. This allows the heat and salinity anomalies to be redistributed over an increasing volume. In our process model, denser waters, unexposed to the surface forcing, are entrained into the mixed layer by the seasonal deepening. However, we assume that in the linear regime, a small surface heat flux perturbation does not lead to a deviation in the mixed layer depth away from the seasonal climatology. In other words, we ignore any anomalous entrainment. We use the non-linear equation of state from the MITgcm to compute the contributions of temperature and salinity to the evolution of the mixed layer density anomaly ρ, that is a nonlinear function of T, S, and the constant pressure p in the surface layer.

Our simple thermodynamic mixed layer model captures the evolution of the surface density anomaly in the Western Subpolar Gyre that arises in response to a summer heat flux perturbation (Fig. 7). We demonstrate that, several months after the perturbation, changes in salinity become the dominant contribution to the density anomaly and over-compensate the temperature contribution. The salinity anomaly evolves non-monotonically both in the MITgcm and in the process model because of the competing effects of surface freshwater fluxes and the seasonal deepening of the mixed layer. By November, we have a decrease in the density of the Subpolar Gyre mixed layer in response to summer cooling (Fig. 8b). This buoyancy anomaly persists into the convective winter months and is communicated to greater depths in the MITgcm (Fig. 8c). Our calculations with the process model remain robust if we increase or decrease the background SST by 1K (not shown). For example, a 1K increase in the assumed climatological temperature shifts the crossover timescale in Fig. 7b one week earlier. These results with the process model suggest a link between air-sea feedback and the seasonality in the AMOC sensitivity to surface heat input.

In contrast to the summer perturbation experiment, the response to an analogous winter cooling in the MITgcm

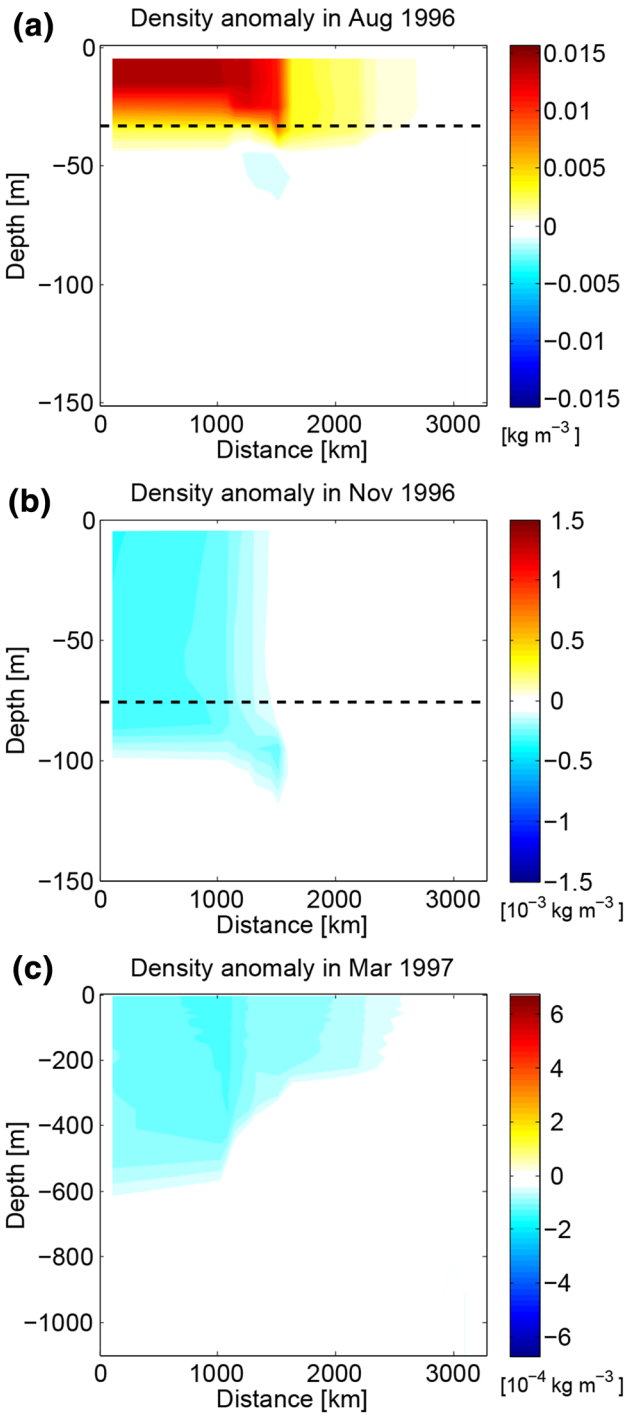

Fig. 8 Evolution of the density anomaly in the MITgcm along a zonal section of the North Atlantic at 57°N after a surface cooling perturbation in July 1996 (as in Fig. 1d). Monthly means for **a** August, 1996; **b** November, 1996; **c** March, 1997. The dashed black line denotes our assumed mixed layer depth in the offline process model. We do not extend our offline process model calculation into the winter months. Note the different vertical axis in **c**

ECCO configuration is marked by a positive mixed layer density anomaly that does not change sign (Fig. 12a). We see that in the case of winter cooling, the density anomaly due to salinity is actually positive and enhances the densification due to temperature. This can be understood in terms of entrainment of high-salinity subsurface waters into the expanding mixed layer as it erodes the halocline beneath. However, it should be noted that the nonlinear effect due to salt entrainment is not captured in the adjoint analysis that linearizes the AMOC sensitivities about the background mixed layer depth. We attempt to identify the dominant factor that explains the difference between the response to summer and winter cooling.

We propose that the shallow mixed layer depth in the summer months is an important factor allowing the transition between a positive and a negative density anomaly in response to summer cooling. We perform additional surface cooling experiments with the process model to illustrate this effect. We keep the same surface heat flux anomaly, background temperature, and boundary conditions as the summer configuration in Fig. 7b. However, instead of assuming an initial summer mixed layer depth of 25 m, we set a constant depth of 300 m (Fig. 13a). In this case, the total density anomaly is smaller compared to the experiment in Fig. 7b, and does not change sign but remains positive.

We also perform a third experiment with the same configuration of the process model. In this experiment, we rescale the heat flux perturbation such that the initial temperature, salinity, and density anomalies are the same as in Fig. 7b, but the mixed layer depth is once again fixed at 300 m. The resulting net density anomaly does not switch sign over the course of 5 months (Fig. 13b) unlike the experiment in Fig. 7b despite the identical background conditions and initial temperature perturbation. This highlights the important role of the shallow summer mixed layer for explaining the negative density anomaly arising in response to summer cooling.

3.2 Impact of air-sea feedback on the response to surface freshwater fluxes

In comparison to surface heat fluxes, the AMOC sensitivity to freshwater fluxes exhibits a weaker seasonality in the simulation with active air–sea feedback (Fig. 2b, blue). We see a small reduction of the already weak seasonality when we fully prescribe the historical surface fluxes (Fig. 2b, orange). Nevertheless, air-sea feedback mechanisms exert a noticeable impact on the AMOC sensitivity to freshwater fluxes over the Subpolar Gyre across all seasons, especially at longer lead times. The AMOC sensitivity to freshwater fluxes with an active bulk formulae parameterization is up to a factor of 2 larger than the corresponding sensitivity in the case of fully prescribed surface forcing (Fig. 2b).

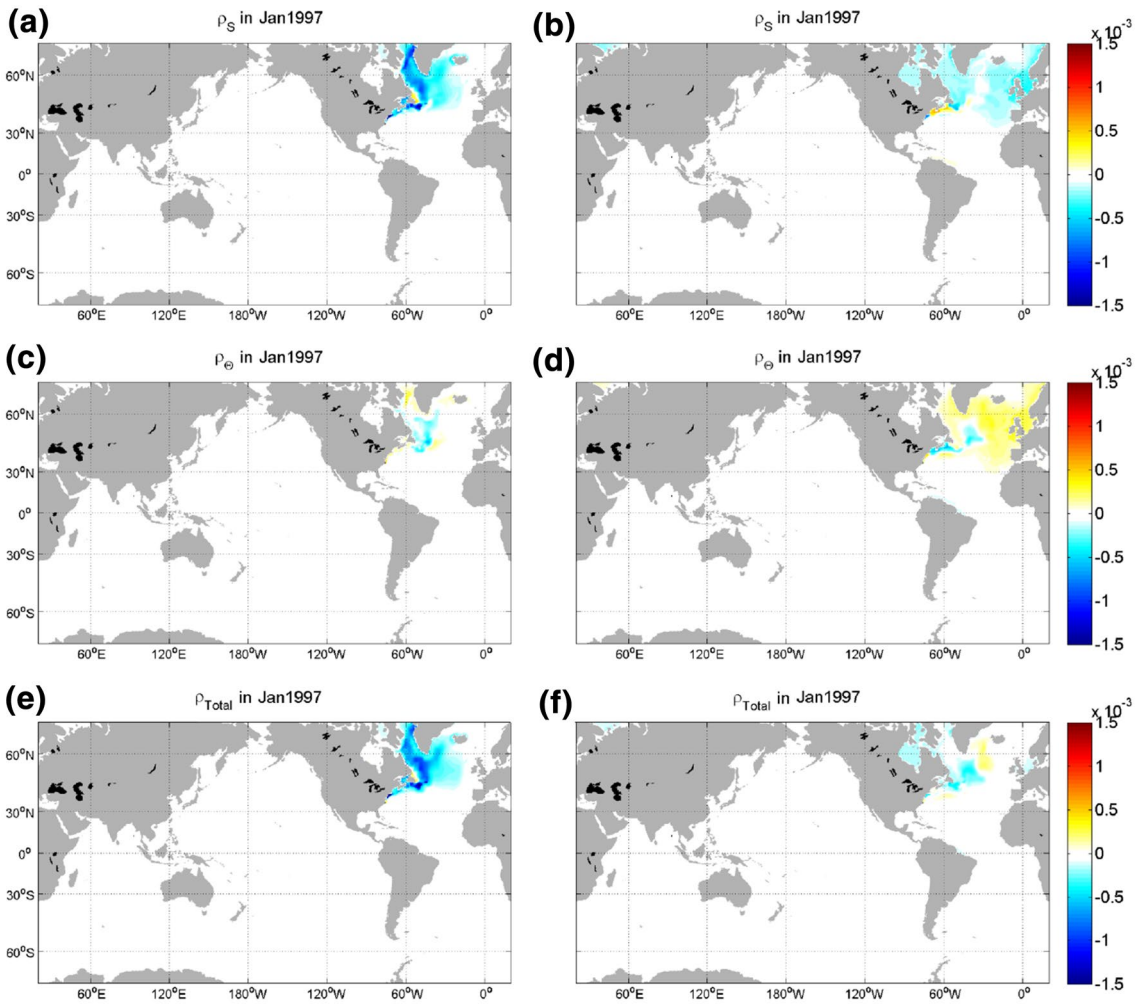

Fig. 9 Density anomalies vertically averaged down to 500 m. Contributions due to salinity (**a**, **b**), temperature (**c**, **d**) and total density anomalies (**e**, **f**) one year after a freshwater flux perturbation applied in January 1996. Left column: experiment with interactive air-sea feedback (**a**, **c**, **e**). Right: experiment with fully prescribed surface fluxes (**b**, **d**, **f**)

We use results from our forward North Atlantic freshwater-hosing experiments to delve into the physical processes through which air-sea feedback modulates the AMOC response to surface freshwater fluxes. We impose a surface freshening in January 1996 that has the same Gaussian spatial pattern as the perturbation in our heat flux experiments. On a timescale of months, by January 1997, the freshwater-hosing of the Subpolar Gyre triggers a weakening of the northward transport of warm highly saline water into the Labrador Sea. This dynamical mechanism gives rise to further freshening and at the same time a cooling of the Western Subpolar Gyre. In the case of parameterized surface fluxes, the negative SST anomaly leads to a reduction in evaporation that amplifies the salinity anomaly (Fig. 9, compare a and b). On the other hand, the active air-sea feedback mechanisms dampen the negative temperature anomaly (Fig. 9b, c). As a result, in the simulation with parameterized air-sea feedback mechanisms, we ultimately see an enhanced freshening that dominates the total density anomaly in the upper layers of the Western Subpolar Gyre affecting both the magnitude and the spatial pattern of the anomaly (Fig. 9e).

In contrast, when we fully prescribe the surface heat and freshwater fluxes, these positive air-sea feedback mechanisms are absent. The local freshening is not amplified by a reduction in evaporation. Moreover, the dynamically-induced cooling of the Labrador Sea partially compensates the density anomaly due to the freshening (Fig. 9b, d, f). Hence, when we perform our hosing experiment in a simulation with prescribed surface fluxes, we obtain a density anomaly that is roughly a factor of 2 smaller than the case with active parameterized fluxes (Fig. 9, compare e and f). This is consistent with the factor of ~2 difference between the corresponding adjoint results for the AMOC sensitivity to freshwater forcing (Fig. 2b). However, some of this

difference may be attributed to the model drift that arises when we switch from parameterized hourly surface fluxes to fully prescribed monthly-mean net fluxes.

In order to avoid the interference of model drift, we once again turn our attention to the experiment where surface flux parameterizations are active in the forward calculation but are not differentiated. When we eliminate the contribution of local air-sea feedback mechanisms, the AMOC sensitivity to surface freshwater fluxes over the Subpolar Gyre does not change at short lead times of ~ 2 years (Fig. 2b, green). However, at lead times longer than 7 years, removing the contribution due to surface feedback noticeably reduces the sensitivity (Fig. 2b). Thus, our results further highlight the important role of air-sea feedback mechanisms in setting the AMOC response to freshwater fluxes. Finally, if we rescale the sensitivity to surface freshwater fluxes into the same units as the sensitivity to surface heat fluxes, the two curves become close to identical at all lead times (compare the green and the brown curve in Fig. 2d). Therefore, we attribute the difference between the AMOC sensitivity to heat fluxes and freshwater fluxes over the Subpolar Gyre (Fig. 2, blue curves in a and b) to the different impact of air-sea feedback mechanisms on these surface fluxes.

4 Discussion and conclusions

Our results suggest seasonal differences in the AMOC sensitivity to surface heat flux anomalies that affect the representation of the overturning circulation and its variability in ocean models. It has been widely accepted that in the winter, when deep water forms, anomalous surface cooling in the Subpolar Gyre strengthens the subtropical AMOC [within a range of time lags, e.g., Pillar et al. (2016)]. However, we find that surface heat loss over the Subpolar Gyre in the summer may have the opposite effect: it can cause a delayed weakening of the AMOC at 26°N. The AMOC response to summer heat flux perturbations is not a mirror image of the response to winter heat flux anomalies. In addition to the sign difference, the magnitude of the AMOC sensitivity to summer heat flux anomalies is smaller than the sensitivity to anomalies in the winter. In contrast, the AMOC sensitivity to freshwater fluxes does not exhibit any seasonal sign reversal.

We find that, to leading order, the seasonality of the AMOC sensitivity to heat fluxes is not due to a dynamical mechanism involving the ocean circulation. Mixed layer thermodynamics and local air-sea feedback processes govern these seasonal differences. Surface cooling of the Subpolar Gyre leads to a reduction in evaporation sustained over several months after the heat flux anomaly has vanished. At the same time, the ocean heat anomaly is efficiently damped by the atmosphere in the summer months when the mixed layer is shallow. As a result, the response to surface heat loss from the Subpolar Gyre in July is a sustained freshening and a buoyancy increase that enhances stratification and weakens the AMOC. In contrast, the response to heat loss in the winter is dominated by the thermal contribution to buoyancy. The heat anomaly in the winter is not trapped near the surface but distributed across a deeper mixed layer and has a smaller impact on SST. Hence, in wintertime both the atmospheric damping of the heat anomaly and the response of surface freshwater fluxes are weaker. The mixed layer depth is the dominant factor setting the different seasonal responses. In addition, the adjustment of surface freshwater fluxes to heat loss in the winter is smaller because of the nonlinearity in the Clausius-Clapeyron relation and the reduced atmospheric humidity in that season.

The AMOC sensitivity to surface freshwater fluxes over the Subpolar Gyre exhibits much weaker seasonality. The air-sea feedback mechanisms are not triggered directly by surface salinity. Nevertheless, air-sea feedback does play an important role in setting the AMOC response to surface freshwater fluxes. Freshening in the Subpolar Gyre constitutes a negative buoyancy anomaly that causes a reduction in the northward oceanic transport of warm high salinity water into the Labrador Sea (see Williams et al. (2015) for a discussion of the AMOC and its role in Labrador Sea heat convergence). Interactive surface fluxes then respond to the resulting SST anomaly and exert a positive feedback on the density anomaly of the Subpolar Gyre mixed layer. They dampen the ocean heat anomaly while at the same time enhancing the salt anomaly via changes in evaporation. Hence, air-sea feedback ultimately amplifies the AMOC response to surface freshwater fluxes.

We thus point out a strong coupling between the parameterized surface heat and freshwater fluxes. Even if a given surface heat flux anomaly is not caused by changes in latent heat, it can impact freshwater fluxes. In turn, salinity perturbations also trigger a chain of mechanisms leading to a response in surface heat fluxes. This has important implications for the buoyancy budget of the Subpolar Gyre mixed layer and for ocean stratification. We infer that air-sea exchange of heat and freshwater cannot be treated as independent drivers of AMOC variability. This poses a challenge for the attribution of historical buoyancy-driven AMOC trends.

Various limitations to our analysis stem from the need to parameterize unresolved processes such as eddy transport and subgridscale mixing, and our reliance on bulk formulae to represent surface heat and freshwater fluxes. Thus, the response to any forcing we apply ultimately depends on the model parameterizations that are also reflected in the adjoint of the GCM. Our results may therefore be very sensitive to the model configuration. For instance, Czeschel et al. (2010) and Pillar et al. (2016) perform adjoint experiments with different configurations of the MITgcm and find a decadal sign

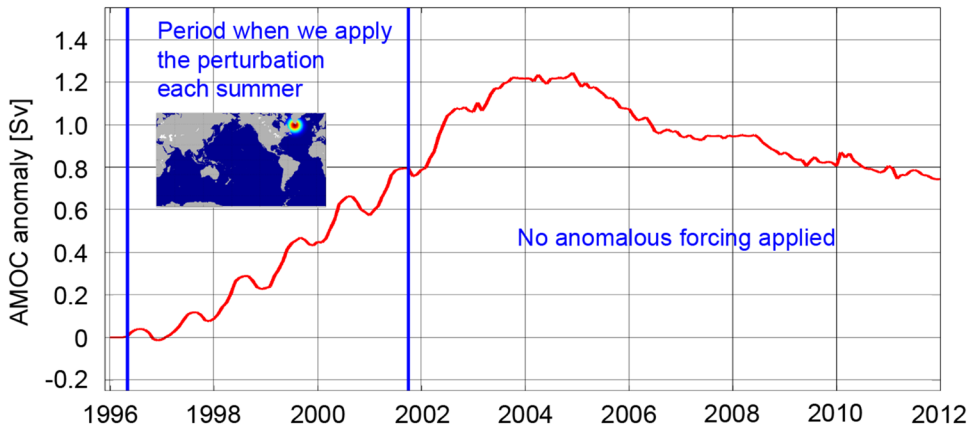

Fig. 10 Response of the AMOC to a sustained surface warming flux applied over the Western Subpolar Gyre repeatedly every summer between 1996 and 2001. The inset map shows the spatial pattern of the applied perturbation with a maximum amplitude off the southern tip of Greenland that is 60 times larger than in Fig. 1d

reversal in the AMOC sensitivity to both surface heat and surface freshwater fluxes. Pillar et al. (2016) fully prescribe surface fluxes, which is analogous to our configuration without parameterized fluxes (orange lines in Fig. 2a, b) and our configuration without differentiation of the bulk formulae (green lines in Fig. 2a, b). Yet, unlike Pillar et al. (2016), we find no decadal sign reversal in the heat flux sensitivity in either of our configurations. A major difference between our study and Czeschel et al. (2010) and Pillar et al. (2016) is that they relax the surface temperature and salinity, as well as the interior fields at 70°N, to seasonal climatology. Pillar et al. (2016) also deactivate the eddy parameteriziation scheme in their adjoint experiments. The difference between our results and Pillar et al. (2016) or Czeschel et al. (2010) demonstrates that model configuration can strongly affect the decadal AMOC response to surface buoyancy flux anomalies over the Subpolar Gyre.

Both our adjoint calculations and our finite perturbation experiments have a limited scope. Our results are valid within a small range of deviations from the background seasonal state (see supplementary Figure 14 in Appendix 3 demonstrating this nonlinearity). Thus we cannot predict how the AMOC would respond to large perturbations that bring the system to a qualitatively different regime, e.g., a shutdown of the AMOC. In addition, our adjoint calculations ignore potentially large changes in nonlinear processes such as convective adjustment. At each time step, our algorithmic differentiation linearizes about a particular convective state of the ocean.

However, the nonlinearity in the AMOC sensitivity to heat fluxes does not imply that our linear sensitivity results are inconsequential. If we impose a surface warming flux over the Western Subpolar Gyre repeatedly every summer over the course of 5 years, we obtain a significant *strengthening* of the AMOC at 26°N (Fig. 10), in agreement with the seasonal sign reversal in our linear sensitivity analysis. The magnitude of the imposed heat flux is 60 times greater than the one in Fig. 1 and hence, an order of magnitude larger than the typical monthly mean heat flux variability in the summer. The resulting strengthening is ≈ 0.13 Sv/year. That is approximately a quarter of the observed 2004-2012 weakening trend of 0.54 Sv/year at the RAPID Array (Smeed et al. 2014). This indicates that sustained seasonal heat flux perturbations can build up over time to yield a substantial AMOC drift.

Finally, no matter what boundary conditions are used in an ocean-only GCM, this cannot make up for the lack of atmospheric coupling. In the real world and in coupled models, the atmospheric circulation adjusts to changes in SST and provides a feedback on the forcing experienced by the ocean (Czaja and Frankignoul 2002; Frankignoul 1985; Danabasoglu 2008; Gastineau et al. 2012; Msadek and Frankignoul 2009; O'Reilly et al. 2016; Timmermann et al. 1998). Feedback from atmospheric dynamics may affect the seasonal differences in AMOC sensitivity to surface heat fluxes. Thus, future studies should explore the seasonality of the AMOC sensitivity to surface heat fluxes in a large ensemble of experiments with a fully-coupled GCM. In addition, we reserve exploring the causal connection between density anomalies in the Subpolar Gyre and the AMOC response in the subtropics for a future study.

Nevertheless, it is important that we have isolated mechanisms that involve local air-sea feedback and cause seasonal differences in the AMOC response to surface heat fluxes. The same set of air-sea interaction processes that we identify in our ocean-only configuration are also present in the coupled system even though atmospheric dynamics may provide an additional positive or negative feedback. Therefore, our results are a step towards explaining the full set of mechanisms that govern the sensitivity of the AMOC to surface buoyancy forcing and the essential role of air-sea feedback.

Acknowledgements The MITgcm source code and instructions are available online at mitgcm.org. The ECCO v4 optimized forcing and initial conditions can be downloaded from www.ecco-group.org. Y.K., D.P.M., and H.L.J. were funded by the OSNAP project through NERC grant, NE/K010948/1. We thank Patrick Heimbach, Gael Forget,

Timothy Smith, Nora Loose, Helen Pillar, Laure Zanna, Dan Jones, and Tom Haine for the helpful discussions regarding ECCO, algorithmic differentiation, and idealized modeling. We thank two anonymous reviewers for their detailed feedback that greatly improved the manuscript.

Appendix 1: Climatological variability of surface heat fluxes

We compare the heat flux anomalies from our forward perturbation experiments to typical variability in the summer and winter seasons. We consider the monthly mean surface heat fluxes over the Subpolar Gyre and compute their standard deviations across all Januaries and all Julys of the historical ECCO simulations (Fig. 11). The summer variability is similar to our imposed perturbation corresponding to Fig. 1a, d. The variability in surface heat fluxes is an order of magnitude larger when we compare winter months across different years.

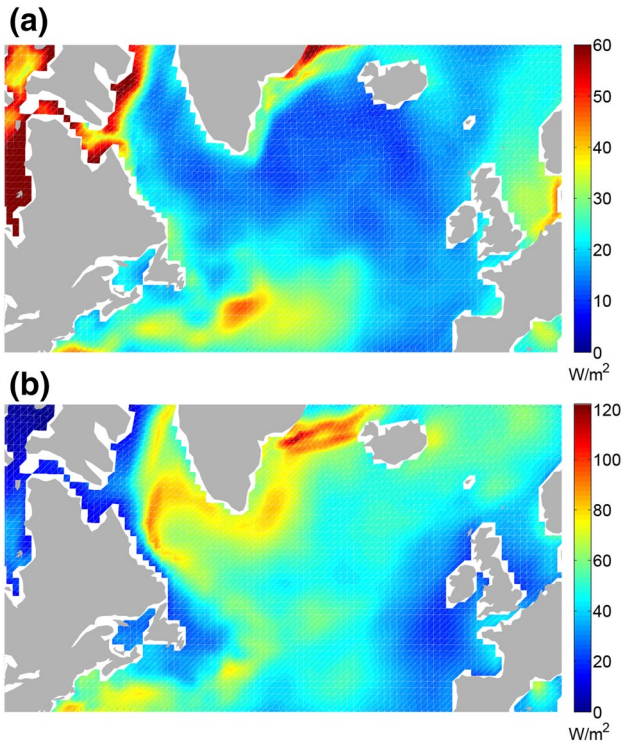

Fig. 11 Standard deviation of the monthly-mean heat flux anomaly relative to the climatological monthly mean across all **a** Julys; **b** Januarys in the ECCO historical simulation. Note the different colorbars

Appendix 2: Local response to surface heat fluxes under deep mixed layer conditions

We explore the local mixed layer density anomalies that arise in the Subpolar Gyre in response to surface heat flux perturbations if the mixed layer depth is large. We first consider a forward experiment with the MITgcm where a surface cooling is applied in January 1996 (Fig. 12a), a winter month marked by mixed layer depths larger than the annual mean and conditions that favor convective mixing. Similarly, we consider a summer experiment with a very large surface cooling (70 times larger than the one in Fig. 1a) and analyze the local response (Fig. 12b) in the MITgcm. Even though the experiment in Fig. 12b begins in July, when the background mixed layer is shallow, the mixed layer depth itself increases in response to the large cooling perturbation. Both the winter cooling experiment and the large summer cooling case exhibit a densification of the upper ocean and no sign change in the density anomaly with time (Fig. 12). In addition, both experiments show salinity entrainment into the deepening mixed layer. The effect of this entrainment is that the salinity contribution to the density budget is positive across all months in the winter case and over the first two months in the summer experiment.

Both experiments in Fig. 12 are influenced by the effective heat capacity of the mixed layer, by nonlinearity in the bulk formulae parameterization, and by vertical entrainment. Our process model helps us disentangle the dominant factors that make the local response to surface heat fluxes different when the mixed layer depth is large. We perform additional calculations with the process model where we keep summer background conditions and apply a surface cooling perturbation as in Fig. 1a but we fix a constant mixed layer depth of 300 m. We first consider a test case (Fig. 13a) where the surface heat flux perturbation has the exact same magnitude as in Fig. 7. However, this triggers a different initial temperature anomaly because the mixed layer is an order of magnitude deeper compared to Fig. 7. Similarly, we consider an analogous test case but with a surface heat flux perturbation whose magnitude is rescaled, so that the initial temperature is the same as in Fig. 7. Both experiments (Fig. 13a and b) demonstrate that the effective heat capacity of the mixed layer is a dominant factor explaining the difference in the response of the local density budget to summer and winter cooling perturbations.

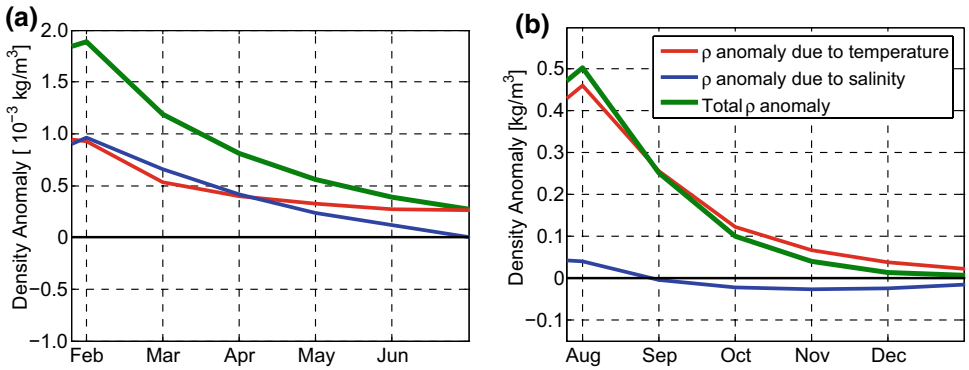

Fig. 12 Contributions to the density anomaly in the upper 30 m of the Western Subpolar Gyre: **a** in the January 1996 heat flux experiment (Fig. 7); The imposed heat flux perturbation is the same as in Fig. 7; **b** in a July 1996 heat flux experiment with a magnitude 70 times larger than in Fig. 7. Monthly mean diagnostics from the MITgcm. Red: density anomaly due to temperature; blue: density anomaly due to salinity; green: total density anomaly based on the full nonlinear equation of state

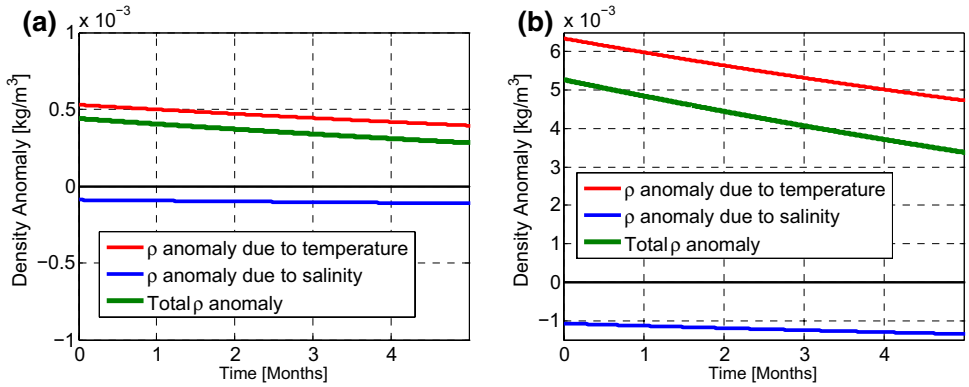

Fig. 13 **a** Contributions to the density anomaly in the process model in a July 1996 heat flux calculation with the same flux perturbation magnitude as in Fig. 7 but a constant mixed layer depth of 300 m. Red: density anomaly due to temperature; blue: density anomaly due to salinity; green: total density anomaly based on the full nonlinear equation of state; **b** same as in **a** but with a flux perturbation rescaled such that the initial temperature, salinity, and density anomalies are the same as in Fig. 7. Notice the different vertical axes in **a** and **b**

Appendix 3: Nonlinearity in the forward heat flux experiments

In order to probe the nonlinear impact of surface heat fluxes on the AMOC, we conduct additional forward perturbation experiments with imposed heat flux anomalies over the subpolar North Atlantic. We compare the response to summer cooling perturbations of various magnitude. We first apply a July heat flux anomaly with the same pattern as in the Fig. 1 experiment but with a magnitude that is 30 times larger (Fig. 14a). This perturbation is an order of magnitude larger than the typical monthly-averaged summer heat flux variability in the region. The applied perturbation induces a more negative AMOC anomaly, consistent with the sign of the results from our adjoint sensitivity analysis. However, if we impose a summer cooling of magnitude 90 times larger than the Fig. 1 perturbation, we see an AMOC response of the opposite sign (Fig. 14a).

If we apply a large enough cooling anomaly, e.g., 100 times larger than the perturbation in Fig. 1, we always see a delayed strengthening of the AMOC at 26°N, no matter if the perturbation is imposed in January or in July (Fig. 14b). This result indicates no seasonal sign reversal in the AMOC sensitivity to large surface heat flux anomalies and can be understood in terms of mixed layer depth modulation. When we impose a substantial cooling perturbation over the Subpolar Gyre in the summer, this leads to a deepening of the mixed layer and a redistribution of the heat anomaly over a larger volume. The increase in effective heat capacity means that the SST anomaly—that triggers air-sea feedback—does not change linearly with the amount of heat. In addition, the mixed layer deepening under a large summer cooling perturbation leads to entrainment of subsurface waters with a higher salt content, which

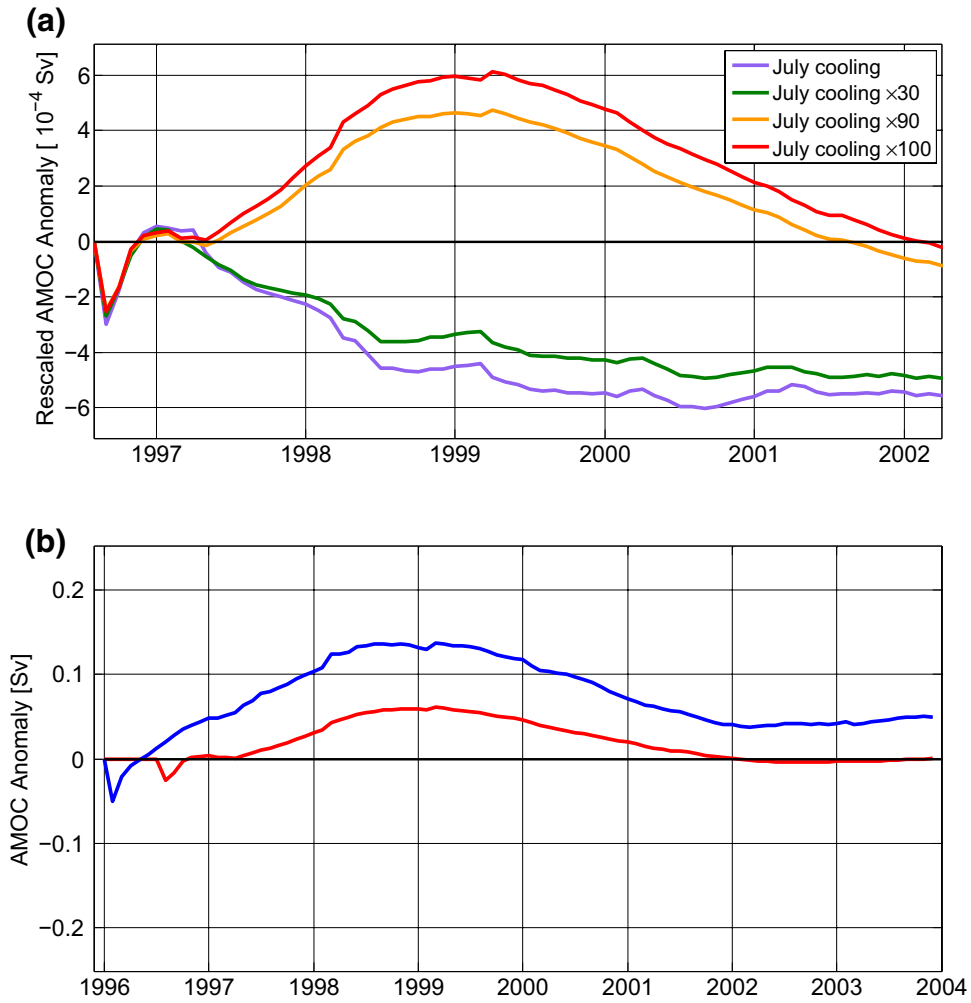

Fig. 14 **a** Response of the AMOC to a surface cooling flux perturbation over the Western Subpolar Gyre with the same pattern and magnitude as in Figs. 1 and 4; or the same pattern but with magnitude rescaled by different constant factors μ. The AMOC anomalies are shown rescaled by $1/\mu$; **b** response of the AMOC to the same surface cooling as in the ×100 case in panel **a** but with a heat flux perturbation applied in January 1996 (blue). The red curve from **a** is replicated for comparison. The AMOC anomalies in **b** are shown unrescaled

exerts a positive feedback on the initial density anomaly (Fig. 13b). The increase in mixed layer heat capacity and the entrainment of salt facilitate a net densification of the upper ocean at a lag of several months in response to a large summer cooling anomaly. This is reminiscent of the winter response, where a surface cooling triggers an increase in the mixed layer density enhanced by the entrainment of high-salinity subsurface waters (Fig. 13a). We emphasize that a nonlinear regime does not have to be triggered solely by a large heat flux anomaly. Any combination of heat and freshwater fluxes that substantially changes the mixed layer depth relative to the seasonal climatology will yield a nonlinear AMOC response.

References

Arzel O, Huck T, Colin de Verdière A (2006) The different nature of the interdecadal variability of the thermohaline circulation under mixed and flux boundary conditions. J Phys Oceanogr 36:1703–1718. https://doi.org/10.1175/JPO2938.1

Buckley MW, Marshall J (2016) Observations, inferences, and mechanisms of Atlantic meridional overturning circulation variability: a review. Rev Geophys 54:5–63. https://doi.org/10.1002/2015RG000493

Bugnion V, Hill C, Stone PH (2006a) An adjoint analysis of the meridional overturning circulation in an ocean model. J Clim 19:3732–3750. https://doi.org/10.1175/JCLI3787.1

Bugnion V, Hill C, Stone PH (2006b) An adjoint analysis of the meridional overturning circulation in a hybrid coupled model. J Clim 19:3751–3767. https://doi.org/10.1175/JCLI3821.1

Cheng W, Chiang JCH, Zhang D (2013) Atlantic meridional overturning circulation (AMOC) in CMIP5 models: RCP and historical simulations. J Clim 26(18):7187–7197. https://doi.org/10.1175/JCLI-D-12-00496.1

Czaja A, Frankignoul C (2002) Observed Impact of Atlantic SST Anomalies on the North Atlantic Oscillation. J Clim 15:606–623. https://doi.org/10.1175/1520-0442(2002)015<0606:OIOASA>2.0.CO;2

Czeschel L, Marshall DP, Johnson HL (2010) Oscillatory sensitivity of Atlantic overturning to highlatitude forcing. Geophys Res Lett 37:L10601. https://doi.org/10.1029/2010GL043177

Forget G, Campin JM, Heimbach P, Hill CN, Ponte RM, Wunsch C (2015) ECCO version 4: an integrated framework for non-linear

inverse modeling and global ocean state estimation. Geosci Model Dev 8:3071–3104
Fukumori I, Wang O, Fenty I, Forget G, Heimbach P, Ponte RM (2017) ECCO Version 4 Release 3. http://hdl.handle.net/1721.1/110380, doi:1721.1/110380
Frankignoul C (1985) Sea surface temperature anomalies, planetary waves, and air-sea feedback in the middle latitudes. Rev Geophys 23(4):357–390. https://doi.org/10.1029/RG023i004p00357
Danabasoglu G (2008) On multidecadal variability of the Atlantic Meridional Overturning Circulation in the Community Climate System Model version 3. J Clim 21(21):5524–5544. https://doi.org/10.1175/2008JCLI2019.1
Gaspar P, Grégoris Y, Lefevre J-M (1990) A simple eddy kinetic energy model for simulations of the oceanic vertical mixing: tests at station papa and long-term upper ocean study site. J Geophys Res 95:16179–16193. https://doi.org/10.1029/JC095iC09p16179
Gastineau F D'Andrea, Frankignoul C (2012) Atmospheric response to the North Atlantic Ocean variability on seasonal to decadal time scales. Clim Dyn 40:2311–2330. https://doi.org/10.1007/s00382-012-1333-0
Giering R (2010) Transformation of algorithms in Fortran Version 1.15 (TAF Version 1.9.70). FastOpt
Gregory JM et al (2005) A model intercomparison of changes in the Atlantic thermohaline circulation in response to increasing atmospheric CO2 concentration. Geophys Res Lett 32:L12703. https://doi.org/10.1029/2005GL023209
Griffies SM (1998) The Gent-McWilliams skew flux. Journal of Physical Oceanography 28:831–841. 10.1175/1520-0485(1998) 028<0831:TGMSF>2.0.CO;2
Griffies SM, Tziperman E (1995) A linear thermohaline oscillator driven by stochastic atmospheric forcing. J. Clim. 8(10):2440–2453. 10.1175/1520-0442(1995) 008<2440:ALTODB>2.0.CO;2
Heimbach P (2008) The MITgcm/ECCO adjoint modelling infrastructure. CLIVAR Exchanges, No. 13, International CLIVAR Project Office, Southampton, United Kingdom, 13-17
Heimbach P, Wunsch C, Ponte R, Forget G, Hill C, Utke J (2011) Timescales and regions of the sensitivity of Atlantic meridional volume and heat transport: toward observing system design. Deep-Sea Res II 58:1858–1879. https://doi.org/10.1016/j.dsr2.2010.10.065
Holdsworth AM, Myers PG (2015) The influence of high-frequency atmospheric forcing on the circulation and deep convection of the Labrador Sea. J Clim 28(12):4980–4996. https://doi.org/10.1175/JCLI-D-14-00564.1
Johnson HL, Marshall DP, Johnson HL, Marshall DP (2002) A theory for the surface Atlantic response to thermohaline variability. J Phys Oceanogr 32(4):1121–1132. 10.1175/1520-0485(2002) 032<1121:ATFTSA>2.0.CO;2
Jones D, Forget G, Sinha B, Josey SA, Boland E, Meijers AJS, Shuckburgh E (2018) Local and remote influences on the heat content of the Labrador Sea: an adjoint sensitivity study. J Geophys Res Oceans 123:2646–2667. https://doi.org/10.1002/2018JC013774
Kawase M (1987) Establishment of deep ocean circulation driven by deep-water production. J. Phys. Oceanogr. 17(12):2294–2317. 10.1175/1520-0485(1987) 017<2294:EODOCD>2.0.CO;2
Kostov Y, Armour KC, Marshall J (2014) Impact of the Atlantic meridional overturning circulation on ocean heat storage and transient climate change. Geophys Res Lett 41:2108–2116. https://doi.org/10.1002/2013GL058998
Lozier MS (2010) Deconstructing the conveyor belt. Science 328(5985):1507–1511. https://doi.org/10.1126/science.1189250
Lozier MS, Gary SF, Bower AS (2013) Simulated pathways of the overflow waters in the North Atlantic: Subpolar to subtropical export, Deep Sea Res., Part II 85:147–153. https://doi.org/10.1016/j.dsr2.2012.07.037
Lozier SM, Bacon S, Bower AS, Cunningham SA, Femke de Jong M, de Steur L, deYoung B, Fischer J, Gary SF, Greenan BJ, Heimbach P, Holliday NP, Houpert L, Inall ME, Johns WE, Johnson HL, Karstensen J, Li F, Lin X, Mackay N, Marshall DP, Mercier H, Myers PG, Pickart RS, Pillar HR, Straneo F, Thierry V, Weller RA, Williams RG, Wilson C, Yang J, Zhao J, Zika JD (2017) Overturning in the subpolar north Atlantic program: a new international ocean observing system. Bull Am Meteorol Soc 98:737–752. https://doi.org/10.1175/BAMS-D-16-0057.1
Marshall JC, Adcroft A, Hill C, Perelman L, Heisey C (1997a) A finite-volume, incompressible Navier Stokes model for studies of the ocean on parallel computers. J Geophys Res 102:5753–5766. https://doi.org/10.1029/96JC02775
Marshall JC, Hill C, Perelman L, Adcroft A (1997b) Hydrostatic, quasi-hydrostatic, and nonhydrostatic ocean modeling. J Geophys Res 102:5733–5752. https://doi.org/10.1029/96JC02776
Marshall J, Scott JR, Armour KC, Campin JM, Kelley M, Romanou A (2014) The ocean's role in the transient response of climate to abrupt greenhouse gas forcing. Clim Dyn 44:2287–2299. https://doi.org/10.1007/s00382-014-2308-0
Marshall J, Johnson H, Goodman J (2001) A study of the interaction of the North Atlantic Oscillation with ocean circulation. J Clim 14(7):1399–1421. 10.1175/1520-0442(2001) 014<1399:ASOTIO>2.0.CO;2
Meehl GA et al (2013) Decadal climate prediction: an update from the trenches. Bull Am Meteorol Soc 95:243–267. https://doi.org/10.1175/BAMS-D-12-00241.1
Pillar H, Heimbach P, Johnson H, Marshall D (2016) Dynamical attribution of recent variability in Atlantic overturning. J Clim 29:3339–3352. https://doi.org/10.1175/JCLI-D-15-0727.1
Msadek R, Frankignoul C (2009) Atlantic multidecadal oceanic variability and its influence on the atmosphere in a climate model. Clim Dyn 33:45–62. https://doi.org/10.1007/s00382-008-0452-0
O'Reilly CH, Minobe S, Kuwano-Yoshida A, Woollings T (2016) The Gulf Stream influence on wintertime North Atlantic jet variability. QJR Meteorol Soc 143:173–183. https://doi.org/10.1002/qj.2907
Rugenstein MAA, Winton M, Stouffer RJ, Griffies SM, Hallberg R (2013) Northern high-latitude heat budget decomposition and transient warming. J Clim 26(2):609–621. https://doi.org/10.1175/JCLI-D-11-00695.1
Seager R, Battisti DS, Yin J, Gordon N, Naik N, Clement AC, Cane MA (2002) Is the Gulf Stream responsible for Europe's mild winters? QJR Meteorol Soc 128(586):2563–2586. https://doi.org/10.1256/qj.01.128
Smeed DA et al (2014) Observed decline of the Atlantic Meridional Overturning Circulation 2004 to 2012. Ocean Sci 10(1):29–38. https://doi.org/10.5194/os-10-29-2014
Stolpe M, Medhaug I, Sedláček J, Knutti R (2018) Multidecadal Variability in Global Surface Temperatures Related to the Atlantic Meridional Overturning Circulation. Journal of Climate. 31 https://doi.org/10.1175/JCLI-D-17-0444.1
Sévellec F, Fedorov AV (2012) The leading, interdecadal eigenmode of the Atlantic Meridional Overturning Circulation in a realistic ocean model. J Clim 26(7):2160–2183. https://doi.org/10.1175/JCLI-D-11-00023.1
Timmermann A, Latif M, Voss R, Grotzner RA (1998) Northern hemispheric interdecadal variability: a coupled air-sea mode. J Clim 11:1906–1931. https://doi.org/10.1175/1520-0442-11.8.1906
Williams RG, Roussenov V, Lozier MS, Smith D (2015) Mechanisms of heat content and thermocline change in the subtropical and subpolar North Atlantic. J Clim 29:9803–9815. https://doi.org/10.1175/JCLI-D-15-0097.1
Winton M, Griffies SM, Samuels BL, Sarmiento JL, Frölicher TL (2013) Connecting changing ocean circulation with changing climate. J Clim 26(7):2268–2278. https://doi.org/10.1175/JCLI-D-12-00296.1

Yeager S, Danabasoglu G (2014) The origins of late-twentieth-century variations in the large-scale North Atlantic circulation. J Clim 27(9):3222–3247. https://doi.org/10.1175/JCLI-D-13-00125.1

Weaver AT, Courtier P (2001) Correlation modelling on the sphere using a generalized diffusion equation. QJR Meteorol Soc 127:1815–1846

Zhang R (2010) Latitudinal dependence of Atlantic Meridional Overturning Circulation (AMOC) variations. Geophys Res Lett 37:L16703. https://doi.org/10.1029/2010GL044474

Zou S, Lozier MS (2016) Breaking the linkage between Labrador Sea Water production and its export to the subtropical gyre. Journal of Physical Oceanography. https://doi.org/10.1175/JPO-D-15-0210.1

Zou S, Lozier MS, Buckley M (2019) How is meridional coherence maintained in the lower limb of the Atlantic Meridional Overturning Circulation? Geophys Res Lett 46:244–252. https://doi.org/10.1029/2018GL080958